

# CHANGES OF STRUCTURAL, OPTICAL AND VIBRATIONAL PROPERTIES OF WO<sub>3</sub> POWDERS AFTER MILLING OR MIXING WITH ReO<sub>3</sub>

E. Cazzanelli <sup>1</sup>, C. Vinegoni <sup>2</sup>, G. Mariotto <sup>2</sup>, A. Kuzmin <sup>3</sup> and J. Purans <sup>3</sup>

<sup>1</sup>Istituto Nazionale per la Fisica della Materia and Dipartimento di Fisica,  
Università della Calabria, 87036 Arcavacata di Rende (Cosenza), ITALY

<sup>2</sup>Istituto Nazionale per la Fisica della Materia and Dipartimento di Fisica,  
Università di Trento, 38050, Povo (Trento), ITALY

<sup>3</sup>Institute of Solid State Physics, 8 Kengaraga str., LV-1063 Riga, LATVIA

A Raman spectroscopic study and X-ray diffraction (XRD) characterizations have been carried out from powder samples of commercial WO<sub>3</sub> after milling steps of various strength and duration. A monoclinic to triclinic phase transition occurs for mild treatments, while for longer times of milling the coexistence of more phases is observed, together with a broadening of XRD patterns, due to a decrease of the crystallites size. A blue coloration of freshly ground WO<sub>3</sub> powder develops in correspondence with such structural changes and a strong decrease of the Raman scattered light is observed. Similar findings are a set of mixed samples W<sub>1-x</sub>Re<sub>x</sub>O<sub>3-y</sub>, with x ranging from 0 to 0.9. The frequency of Raman band, associated with the strong tungsten-oxygen bonds at the defective surface of crystalline grains, was found to be different for pure ground powders and mixed samples.

## INTRODUCTION

Tungsten oxide (WO<sub>3</sub>) is by far the most used electrochromic material, and its physical properties have been extensively studied in various crystalline and amorphous phases or in combination with other oxides (1-7). Nevertheless, some interesting aspects of WO<sub>3</sub> phase transitions sequence and of mechanisms of color centers formation remained unsettled. However, it is generally accepted that such defects consist of electron charge excess, localized at the octahedra basic units [WO<sub>6</sub>] (8).

Pure stoichiometric WO<sub>3</sub> crystal is transparent with a band gap about 2.9 eV at room temperature (9), while the commercial powders show a yellow color and exhibit n-type semiconductivity. The oxide develops a blue coloration during the electrochemical insertion of small cations (10,11). The blue color of tungsten oxide can be also induced

by the UV irradiation (12-14) as well as by annealing in vacuum (15). In the latter treatment, a reduction process of  $WO_3$  grain surface leads to color centers formation, but the characteristic blue coloration is fully reversible under thermal annealing combined with the oxidizing action of the normal atmosphere (15). Treatments inducing some degree of amorphisation of the crystalline structure, like ion beam bombardment (16), promote also the change of electronic distribution in the deformed regions and a consequent modification of its optical properties.

An even easier method to modify the  $WO_3$  surface structure, which help the formation of electronically charged defects, is provided by simple mechanical treatments like milling (17,18), but an extensive analysis of the effects as a function of the milling parameters is far from being done.

A different approach to obtain charged defects with specific optical absorption properties exploits the mixing of tungsten oxide with oxides having a different electronic configurations. To this aim, rhenium trioxide appears an interesting candidate, because of its electronic excess with respect to  $WO_3$  configuration. In fact, the addition of even small fractions of  $ReO_3$  to  $WO_3$  powders, causes a strong coloration to occurs in mixtures after a proper thermal treatment.

The aim of the present work is to investigate the structural transformations induced by means of various milling treatments. In particular, the paper will be focused on the transformations associated to color changes, and will compare these optical, structural and vibrational changes with those induced by the high temperature mixing of tungsten oxide with rhenium oxide.

## EXPERIMENTAL

### Sample preparation

The starting material for the present study is a commercial  $WO_3$  powder, with a nominal purity of 99.9%, which appear of a yellow color. In the following this powder will be identified as "virgin" powder. A slightly different material, as demonstrated by our XRD and Raman measurements, discussed later, is the commercial powder which underwent to a mild milling procedure, consisting of a manual compression in a mortar of agate for a few minutes. In the following this kind of powder will be labeled "treated" powder. Strong mechanical treatments have been performed on the "virgin" powder by using a ball milling machine Retschmuele, with three balls of agate having diameters between 0.5 cm and 1 cm and weight between 0.17 g and 1.09 g, working at a frequency of the order of 1 Hz (50-70 cycles per minute) for different times, ranging from a few

minutes up to 21 hours. The samples obtained by means of this treatment will be referred as to "ground powders".

A more complex procedure has been adopted to obtain the "mixed powders", i.e.: different mixtures of  $\text{WO}_3$  and  $\text{ReO}_3$  powder, obtained by oxidizing metallic rhenium and giving XRD pattern similar to those of commercial rhenium trioxide with 99.9% purity. They are indicated by the general formula  $\text{W}_{1-x}\text{Re}_x\text{O}_{3-y}$  where the index  $x$  represents the relative molar fraction of  $\text{ReO}_3$  at the beginning of the mixing process and the index  $y$  reflects the non-stoichiometry of the material (note that the use of this notation does not imply the formation of a new phase of a mixed crystal or a solid solution). The mixed samples were produced from  $\text{WO}_3$  "virgin" powder, as defined before. The starting materials have been finely ground in air by manual grinding for some minutes, and then sealed under vacuum in quartz ampoules which underwent independent cumulative heating for 17 h at  $450^\circ\text{C}$  and then for 73 h at  $600^\circ\text{C}$ . After the thermal treatments, the powders were ground in air once again. Following this procedure seven different compositions have been obtained, ranging from  $x=0.1$  to  $x=0.9$ , whose color varied from grayish-blue to black.

#### Experimental set-up

All the  $\text{WO}_3$  powder samples were analyzed by standard X-ray diffraction (XRD) and Raman spectroscopy. The mixed powders were also studied by X-ray absorption spectroscopy (XAS).

The samples for XRD and XAS have been prepared by deposition on a Millipore filter of the powder from an aqueous suspension driven by a vacuum pump. The X-ray diffractometer was a model Bragg-Brentano, made by ItalStructures, working with the  $\text{CuK}\alpha$  radiation. The X-ray diffractograms were recorded at room temperature in the angle range  $2\theta = 20$ - $65$  degree and a step  $\Delta(2\theta) = 0.05$  degree.

Experimental X-ray absorption spectra of the W and Re  $L_3$ -edge were recorded in transmission mode at the LURE DCI (Orsay, France) storage ring on the EXAFS-3 beam line located at the bending magnet. The DCI storage ring operated at the energy 1.85 GeV and a maximum stored current 316 mA. A standard transmission scheme with a Si(311) double-crystal monochromator and two ion chambers containing argon gas was used. The measurements were done at room temperature. The extended X-ray absorption fine structure (EXAFS), located above the edge, was extracted and analyzed using the "EDA" software package following the standard procedure (19).



Different sample preparation methods have been adopted for the Raman spectroscopic studies; the most effective consisted in a deposition on a microscopy cover glass some droplets of a suspension of  $\text{WO}_3$  powders in acetone. After the necessary time for solvent evaporation the deposited powders show a good adhesion to the substrate and allow for a good Raman signal detection. The room-temperature Raman spectra have been carried out in back-scattering geometry using a micro-Raman set-up, consisting of an Olympus microscope (model BHSM-L-2), mounting an objective 80 $\times$  with a numerical aperture  $N_A = 0.75$ , and coupled to an 1 meter focal length double-pass Jobin-Yvon monochromator (Ramanor, model HG2-S) equipped with holographic gratings (2000 grooves/mm). The spectra were excited by the 530.9 nm line of a Krypton laser, which was operated so that the power entering in the microscope was maintained below 10 mW. The spectral resolution was of the order of 3  $\text{cm}^{-1}$ . The scattered radiation was detected by a cooled (- 35  $^\circ\text{C}$ ) photomultiplier tube (RCA, model C31034A-02), operated in photon counting mode. The signal was stored into a multichannel analyzer and then sent to a microcomputer for the analysis. For the temperature dependence study, the experimental set-up was set in the standard macro-Raman configuration, with a right angle scattering geometry, and the powder samples have been sealed into a quartz square cuvette.

## RESULTS AND DISCUSSION

### Ground powders

A preliminary investigation has been made on the phase transitions sequence of our powder samples, by analyzing the Raman spectra evolution in a wide range of temperatures (down to 32 K and up to 1073 K) and after thermal cycling and mild mechanical treatments. The detailed findings of such investigation will be reported elsewhere, but some results are worth to mention here. First, our powder samples undergo to a phase transition from the monoclinic phase of the "virgin" powders to the triclinic structure ("treated" powders) after quite moderate milling, and even after manual pressure in a mortar of agate; they maintain this latter structure at room temperature for long times. Second, at low temperature ( $T < 250$  K), our samples do not show the transition from the triclinic phase to the second monoclinic phase, of polar and piezoelectric character, reported by Salje for single crystals (20,21). Instead, the Raman spectra give some evidence of a diffuse transition in the range 30-150 K, quite similar to that observed in microcrystals (22,23).

The transformation of the powders from monoclinic to triclinic structure, under weak milling treatment, can be inferred from small modifications of the XRD patterns, but a clearer evidence is given by the evolution of low frequency bands (up to 100  $\text{cm}^{-1}$ )



of the Raman spectra. These bands correspond to lattice modes of librational nature and are noticeably affected by the transitions between the low symmetry phases of  $\text{WO}_3$ , which involve mainly collective rotations of the basic  $[\text{WO}_6]$  octahedral units (2,24). Note that the XRD patterns are more sensitive to the tungsten atoms positions, which negligibly change in the transition. The Raman spectra show different features in the monoclinic and triclinic phases (21): the transformation of the powder samples is reflected by the evolution in the Raman spectrum, in particular by the relative intensity decrease of the  $34\text{ cm}^{-1}$  peak (typical of monoclinic phase) and the simultaneous increase of the  $41\text{ cm}^{-1}$  peak (typical of triclinic phase).

Fig. 1 reports various spectra in the range  $20\text{-}100\text{ cm}^{-1}$  of samples which underwent increasing times of grinding. The above mentioned spectral evolution for ground  $\text{WO}_3$ , reflecting the gradual transformation from monoclinic to triclinic phase, is quite similar to that observed, at room temperature, for powder samples after different cooling times (from few minutes up to about two hours) in liquid nitrogen. The transformation induced in such way can be reversed only by thermal annealing process at high temperatures (at least  $> 570\text{ K}$ ). In any case, the  $\text{WO}_3$  powders undergoing mild mechanical treatments do not show evident coloration effect, and the final triclinic phase appears to be well defined, both for XRD and Raman spectroscopy.

A different phenomenology occurs when the mechanical treatments increase in their strength and in their duration. Maintaining always a fixed milling frequency of about  $1\text{ Hz}$ , increasing times of milling have been analyzed: for treatments of the order of 1 hour a change of color is observed, from the pale yellow of the monoclinic or triclinic powders toward a greenish color; a strong blue coloration has reached by increasing the times of milling up to many hours.

The structural evolution for increasing milling times can be observed through the XRD spectra, reported in Fig. 2. Their analysis shows that upon milling the decrease of the crystallite size occurs leading to the strong broadening of the diffraction lines. A similar evidence is contained in the Raman spectral evolution of the ground powders, depicted in Fig. 3. After a first transformation into the triclinic phase, observed for mild mechanical treatments (it can be also seen in Fig. 3 by comparing the first spectrum of the "virgin" powders with the ones undergoing the shortest milling treatments), the low frequency Raman peaks broaden remarkably for higher milling times, in such a way to make impossible the assignment to a well defined crystal phase. It is interesting to note that in some step of the structural evolution (sample after 1 h milling) new peaks appears as shoulders in various region of the spectrum, at  $143\text{ cm}^{-1}$ ,  $643\text{ cm}^{-1}$  and  $680\text{ cm}^{-1}$ , with frequencies corresponding enough to the ones of the low temperature monoclinic (polar) phase (20,21), which has been not observed in the low temperature spectra collected on the same starting powders. A similar findings of such modes at room temperature is reported for  $\text{WO}_3$  microcrystals of sizes below  $100\text{ nm}$  (22,23).

However, the most striking change in the Raman spectra of the ground powders concerns the strong decrease of the integrated intensity in the spectral range from 20 to 900  $\text{cm}^{-1}$ . This effect seems to be connected to the changes of the optical properties of the powders, rather than to structural transformations. The increase of milling time leads to the bluish coloration of the samples which is consistent with a model of the  $\text{W}^{5+}$  defect formation at the surface of grains. The high surface-to-bulk ratio for the grains of smaller size favors the absorption of the incident and scattered light, thus allowing a much lower amount of the Raman scattered radiation to reach the collection optics.

An interesting spectroscopic evidence of the modification of the grains surface upon milling is provided by the Raman band centered at about 950  $\text{cm}^{-1}$ , whose relative intensity increases versus the milling duration, as it can be seen in Fig. 4. Such high frequency vibration is characteristic of the strong W-O bonds, and does not exist in the "virgin" powder (see Fig. 4a). It can be attributed to presence of W-O terminal bonds at the grain surfaces and to relaxed environment around  $\text{W}^{5+}$  color centers (6, 25-28).

It should be noted that the deep modifications, induced in the powders by long milling processes, with a decrease of the crystallites size, color changes and strong Raman intensity decrease, are not long-lasting effects, in contrast to the irreversible character of the structural phase transition induced by weak mechanical treatments: after some time, of the order of days or weeks, depending from the amount of the coloration, the modified powders after milling return back to the original color. However the size of the crystallites remains the same. The temperature treatments at about 470 K in the normal atmosphere strongly accelerate this bleaching phenomenon, while similar thermal treatments in inert gases ( $\text{N}_2$  or Argon) maintains the blue coloration invariant. Raman measurements, performed on the ground powders after 6 months in air at room temperature or after some hours in air at very high temperatures (about 1270 K), show a good restoration of the Raman intensity to the values before the milling. The spectral shape becomes also similar to the one of the "virgin" powders only in the case of high temperature annealing.

### Mixed samples

Similar deep color changes, but irreversible against oxidizing atmosphere, have been observed for mixed  $\text{W}_{1-x}\text{Re}_x\text{O}_{3-y}$  samples, which have been studied also by using the same spectroscopic techniques. The mixing of monoclinic tungsten oxide (m- $\text{WO}_3$ ) with cubic rhenium oxide (c- $\text{ReO}_3$ ), followed by high temperature treatment, induces changes in the coloration of the mixture, from the pale yellow typical of bulk  $\text{WO}_3$  toward a grayish-blue coloration, similar to that induced by electrochemical cation intercalation. For very high amounts of rhenium oxide the sample color becomes black.



The strong quenching of the Raman intensity, accompanying the creation of optically absorbing defects, is observed also in the mixed powders (see Fig. 5). The dramatic intensity decrease versus the  $x$  value, observed in the mixtures, cannot be justified by the decreasing content of  $\text{WO}_3$ : in fact, the total Raman intensity strongly decreases of about a factor 20 in passing from the pure  $\text{WO}_3$  to the mixed composition with about 10% rhenium oxide, and a further minor decrease can be estimated when probing compositions with increasing rhenium content. No significant Raman scattering signal can be observed for the sample with  $x=0.9$ .

All the observed vibrational modes in the frequency region  $20\text{-}900\text{ cm}^{-1}$ , for all mixed samples, can be assigned to tungsten oxide dynamics. The Raman spectra in the mixed samples with higher  $x$  seem rather similar to the spectra of monoclinic pure  $\text{WO}_3$  measured at temperatures well above the ambient one. The addition of rhenium oxide does not induce any remarkable change in the spectral shape, like the appearance of new bands. This fact suggests that no chemical reaction or formation of solid solution occur in the bulk of the grains, and the rhenium-rich phase is not Raman active. The XRD spectra, shown in Fig. 6, confirm this assumption. The observed diffraction patterns can be interpreted as a sum of two phases: a pure  $\text{WO}_3$  phase, monoclinic but similar to the high temperature range of this phase, approaching the orthorhombic structure (a XRD evidence supporting this interpretation is the doubling of the relative intensity of the first diffraction peak at  $2\theta = 23^\circ$ ), and a pure  $\text{ReO}_2$  phase with high-temperature rutile-type structure and orthorhombic space group (JCPDS nr.9-274). Some defect of oxygen can be postulated, corresponding to a non-stoichiometry of the order of 2%. Note that the  $\text{ReO}_2$  phase appears in the mixture due to a decomposition of  $c\text{-ReO}_3$  at  $400^\circ\text{C}$  during the sample preparation and, in the pure state, it is stable at temperatures above 570 K. Thus, the positions of all peaks in XRD patterns well correspond to the sum of monoclinic  $\text{WO}_3$  and orthorhombic  $\text{ReO}_2$  and no presence of new phases, due to mixing, was observed.

The last conclusion is fully confirmed by the results of the XAS study at the W and Re  $L_3$ -edges. Opposite to XRD providing the information averaged over the long range order, the XAS is atom site selective and short-range order sensitive that allowed us to probe separately the environment around tungsten and rhenium ions. The experimental extended X-ray absorption fine structure (EXAFS) spectra are shown in Fig. 7. One can see that the noise in experimental data increases with decrease of the ion (W or Re) content. Also a small separation (about 320 eV) between W and Re  $L_3$  edges does not allow to perform accurate analysis of the experimental data however a qualitative conclusion can be withdrawn from comparison with reference materials (pure  $\text{WO}_3$  and  $\text{ReO}_2$ ). In fact, the local environment around tungsten and rhenium ions remains similar at any composition and is close to the one in the reference compounds.



The persistence of the Raman spectrum of "bulk"  $\text{WO}_3$  in all the samples with appreciable signal suggests a model of segregation where particles of pure tungsten oxide, not too much perturbed in its crystal structure, are surrounded by zones of  $\text{ReO}_2$ . The color centers responsible for the optical absorption are preferentially localized on the interfaces between the two materials. The electron excess of Re with respect to W results in that tungsten ions located at the interfaces have the valence state lower than  $6+$ , being the cause of the deep-blue color. In this case the color changes due to the mixing are quite stable and irreversible, against the oxidizing action of the normal atmosphere. This last experimental evidence leads to discard the hypothesis that the coloration is only due to vacuum induced reduction at the high temperatures used during the mixing process (15).

A spectroscopic indication of the presence of deformed  $[\text{WO}_6]$  octahedra is given by the appearance of a Raman band in the range  $950\text{-}1000\text{ cm}^{-1}$  for the mixed samples, as it can be seen in Fig. 8. It is worth to note that the mean frequency of this additional Raman band is about  $980\text{ cm}^{-1}$ , higher than the usual values of about  $950\text{ cm}^{-1}$  observed in the pure ground sample and also reported for tungsten oxide hydrates (29). This difference in the bond strength suggests a slightly different nature of the defects created in the mixed samples at the interface with rhenium oxide.

Except for this difference in the position of the high frequency band at  $\sim 950\text{-}980\text{ cm}^{-1}$ , a general comparative analysis between mixed samples and ground pure  $\text{WO}_3$  suggests that the observed modification of the electronic structure, henceforth of the optical properties of  $\text{WO}_3$ , occurs at the grain boundaries ( $\text{WO}_3/\text{ReO}_2$ ), in the mixed samples, and at the open surface of  $\text{WO}_3$  crystallites, in the case of pure ground powders, while the bulk electronic and vibrational properties of  $\text{WO}_3$  phase remain mainly unchanged, as revealed by the substantial invariance of the Raman spectral shape. This open surface/grain boundaries effects can be well attributed to tungsten ions having the effective charge  $5+$ , whose presence at the surface of pure  $\text{WO}_3$  has been confirmed recently by scanning tunneling microscopy (30).

#### ACKNOWLEDGMENTS

The authors would like to thank Mrs. C. Armellini for the help in preparation of ground  $\text{WO}_3$  samples and XRD measurements, Dr. E. Zanghellini for developing software for Raman data analysis and for useful discussions, Dr. A. Veispals for the preparation of mixed compounds  $\text{W}_{1-x}\text{Re}_x\text{O}_{3-y}$  and Dr. A. DiCicco for supplying with the X-ray absorption spectrum of  $\text{ReO}_2$  reference compound. One of us (J.P.) wish to thank the LURE laboratory (Orsay) for the support of the XAS measurements. A.K. and J.P. are also grateful to the Università di Trento for hospitality and financial support.

## REFERENCES

1. E. Salje, *Ferroelectrics*, **12**, 215 (1976).
2. P.W. Woodward, A.W. Sleight, and T. Vogt, *J. Phys. Chem. Solids*, **56**, 1305 (1995).
3. B.O. Loopstra and H.M. Rietveld, *Acta Crystallogr. B*, **25**, 1420 (1969).
4. E. Salje, *Acta Crystallogr. B*, **33**, 574 (1977).
5. K.L. Kehl, R.G. Hay, and D. Wahl, *J. Appl. Phys.*, **23**, 212 (1952).
6. T. Nanba, Y. Nishiyama, I. Yasui, *J. Mater. Res.*, **6**, 1324 (1991).
7. E.J. Flynn, *Phys. Rev. B*, **21**, 1105 (1980).
8. C.G. Granqvist, *Appl. Phys. A*, **57**, 3 (1993).
9. T. Iwai, *J. Phys. Soc. Jpn.*, **15**, 1596 (1960).
10. S.K. Deb, *Appl. Opt. Suppl.*, **3**, 192 (1969).
11. C.G. Granqvist, *Solid State Ionics*, **53 & 56**, 479 (1992).
12. C. Bechinger, D. Ebner, S. Herminghaus, and P. Leiderer, *Solid. State Comm.*, **89**, 205 (1994).
13. C. Bechinger, G. Oefinger, S. Herminghaus, P. Leiderer, *J. Appl. Phys.* **74**, 4527 (1993).
14. S.K. Deb, *Philos. Mag.*, **27**, 801 (1973).
15. I. Lefkowitz, M.B. Dowell, and M.A. Shields, *J. Solid State Chem.*, **15**, 24 (1975).
16. E. Salje, A.F. Carley, and M.W. Roberts, *J. Solid State Chem.*, **29**, 237 (1979).
17. S. Laruelle and M. Figlarz, *J. Solid State Chem.*, **111**, 172 (1994).
18. S. Begin-Colin, G. Le Caer, M. Zandona, E. Bourzy, and B. Malaman, *J. Alloys and Compounds*, **227**, 157 (1995).
19. A. Kuzmin, *Physica B*, **208 & 209**, 175 (1995); *J. Phys. IV (France)* (1997) (in press).
20. E. Salje and K. Viswanathan, *Acta Crystallogr. A*, **31**, 356 (1975).
21. E. Salje, *Acta Crystallogr. A*, **31**, 360 (1975).
22. M. Arai, S. Hayashi, K. Yamamoto, and S.S. Kim, *Solid State Comm.*, **75**, 613 (1990).
23. S. Hayashi, H. Sugano, H. Arai, and K. Yamamoto, *J. Phys. Soc. Jpn.*, **61**, 916 (1992).
24. R. Diehl, G. Brandt, and E. Salje, *Acta Cryst. B*, **34**, 1105 (1978).
25. G.M. Ramans, J.V. Gabrusenoks, and A.A. Veispals, *Phys. Status Solidi A*, **74**, K41 (1982).
26. M. Pham Thi and G. Velasco, *Solid State Ionics*, **14**, 217 (1984).
27. Y. Shigesato, Y. Hayashi, A. Masui, and T. Haranou, *J. Appl. Phys.*, **30**, 814 (1991).
28. J.V. Gabrusenoks, P.D. Cikmach, A.R. Lusic, J.J. Kleperis, and G.M. Ramans, *Solid State Ionics*, **14**, 25 (1984).
29. M.F. Daniel, B. Desbat, J.C. Lessegues, B. Gerand, and M. Figlarz, *J. Solid State Chem.*, **67**, 235 (1987).
30. J.K. Rawlings, J.S. Foord, P.A. Cox, R.G. Egdell, J.B. Pethica, and B.M.R. Wanklyn, *Phys. Rev. B*, **52**, R143 (1995).

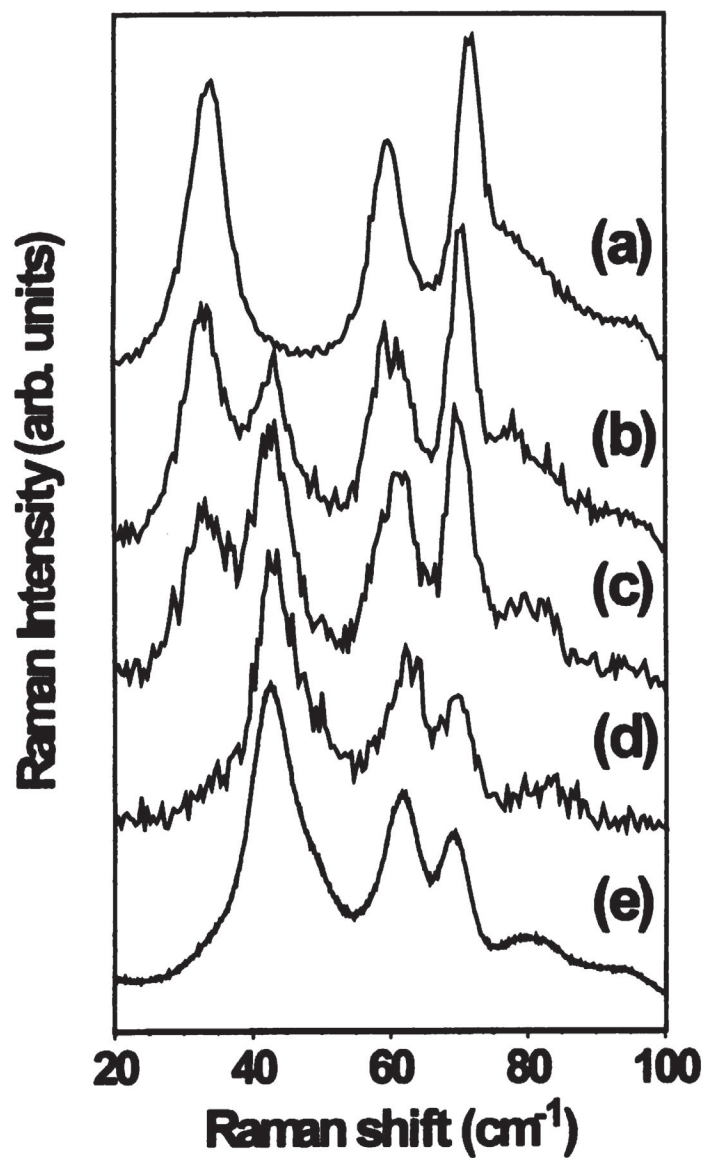


Fig. 1. Raman spectra of tungsten oxide collected in the range 20-100  $\text{cm}^{-1}$  from (a) reference "virgin" powder, monoclinic structure, (b) the same powder after manual pressure for 5 s, (c) manual pressure for 10 s (d) 2 min, (e) reference "treated" powder, triclinic.



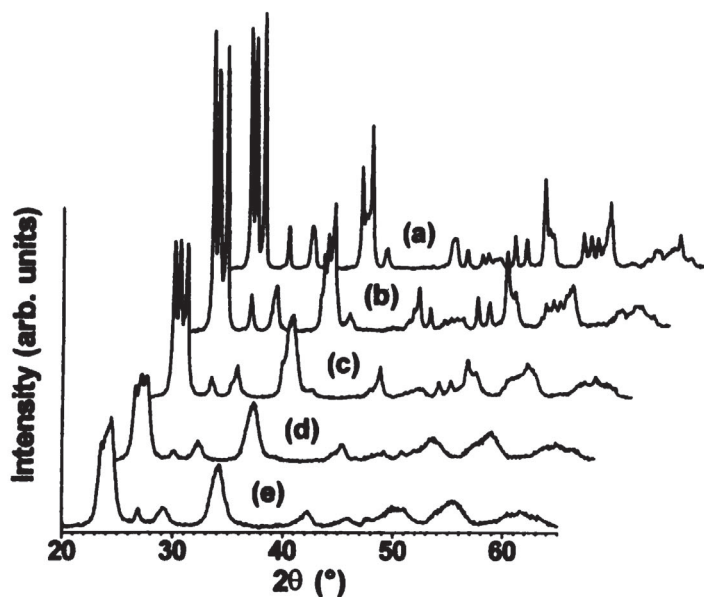


Fig. 2. XRD patterns of tungsten oxide powder as a function of the milling time: (a) "virgin" powder, (b) 2 min milling, (c) 15 min milling, (d) 2 h milling, (e) 21 h milling.

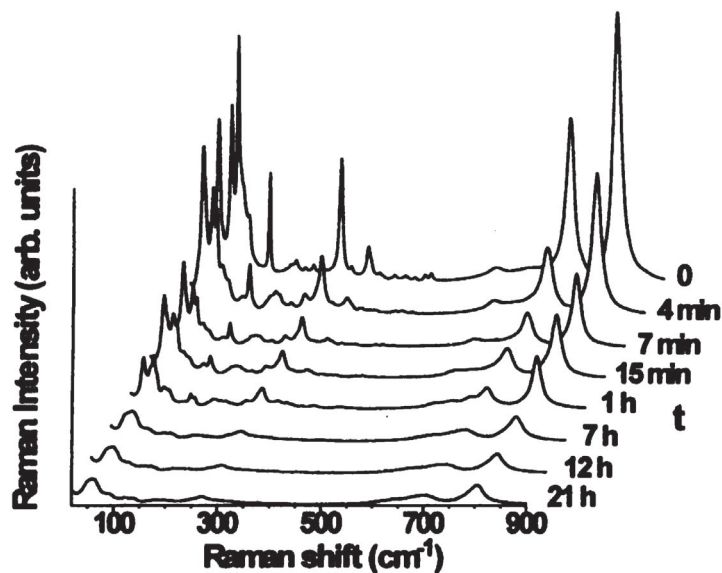


Fig. 3. Total Raman spectra of  $\text{WO}_3$  (frequency range 20-900  $\text{cm}^{-1}$ ) as a function of the milling time  $t$ . Exciting wavelength 530.9 nm. Note that the spectrum at  $t=0$  corresponds to the "virgin"  $\text{WO}_3$  (see experimental section for details).

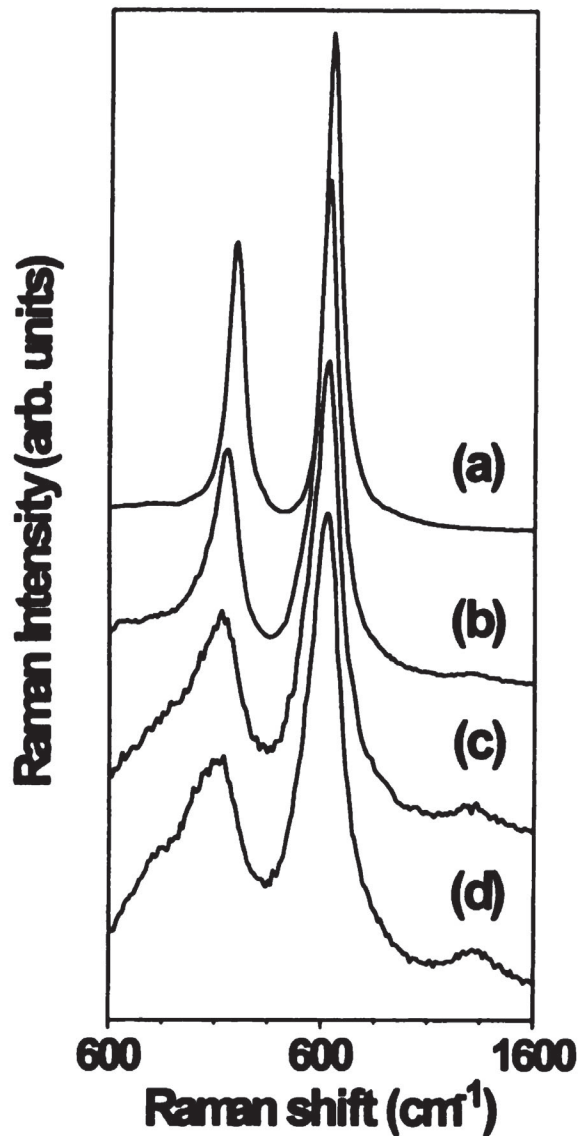


Fig. 4. Variation of the Raman band at  $950\text{ cm}^{-1}$  in ground  $\text{WO}_3$  powders as a function of milling time in comparison with the stretching modes at  $800\text{ cm}^{-1}$  and  $710\text{ cm}^{-1}$ : (a) "virgin" powder, (b) 15 min milling, (c) 2 h milling, (d) 21 h milling.

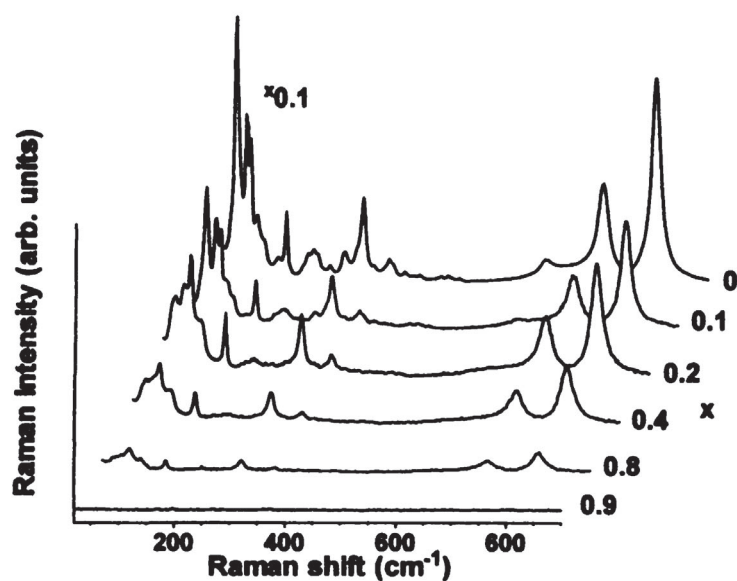


Fig. 5. Raman spectra of  $W_{1-x}Re_xO_{3-y}$  mixed compounds for various compositions  $x$ . The top spectrum is plotted on a full scale 10 times larger than the other spectra. Exciting wavelength 530.9 nm. Note that the spectrum at  $x=0$  corresponds to the "treated"  $WO_3$  (see experimental section for details).

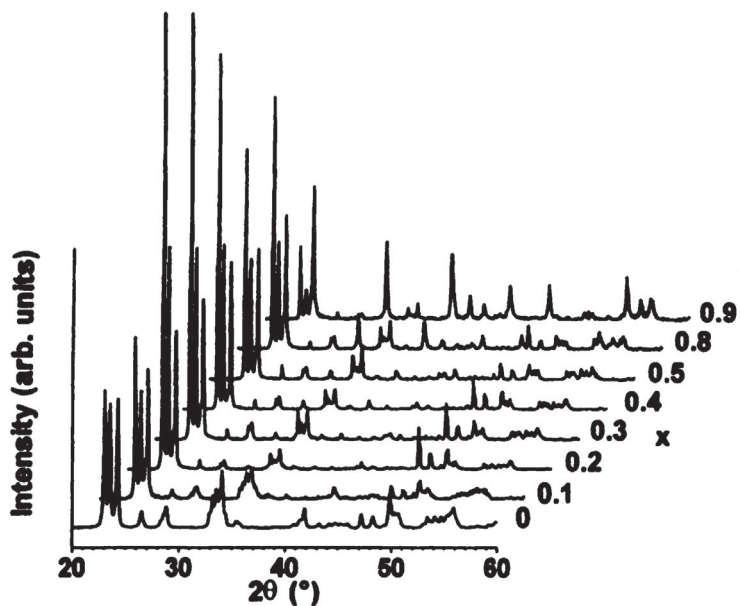


Fig. 6. XRD spectra of  $W_{1-x}Re_xO_{3-y}$  mixed compounds for various compositions.



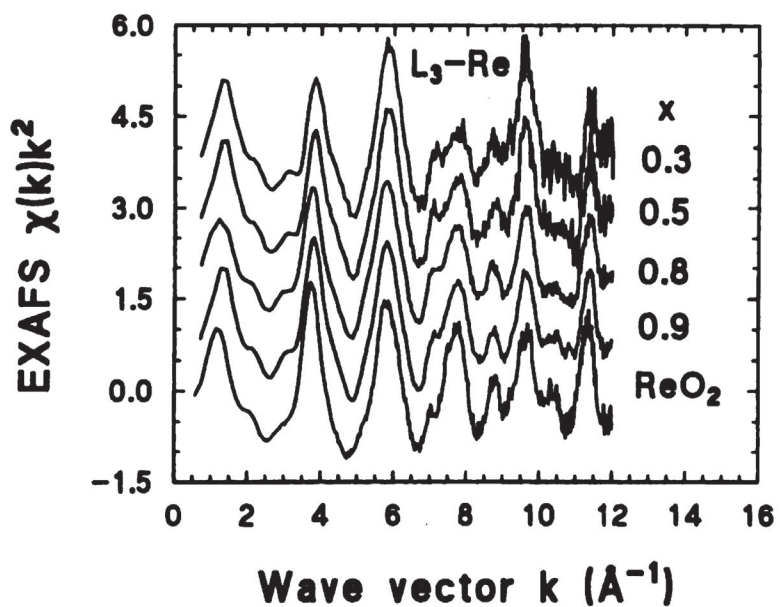
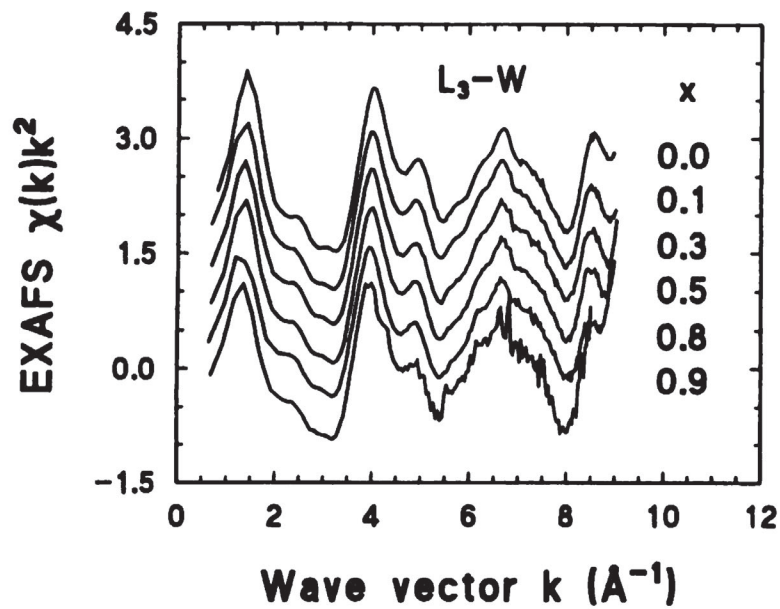


Fig. 7. Experimental EXAFS  $\chi(k)k^2$  spectra of the W and Re  $L_3$ -edge in  $W_{1-x}Re_xO_{3-y}$  mixed compounds. The data for pure  $WO_3$  ( $x=0$ ) and  $ReO_2$  crystals are shown for comparison.

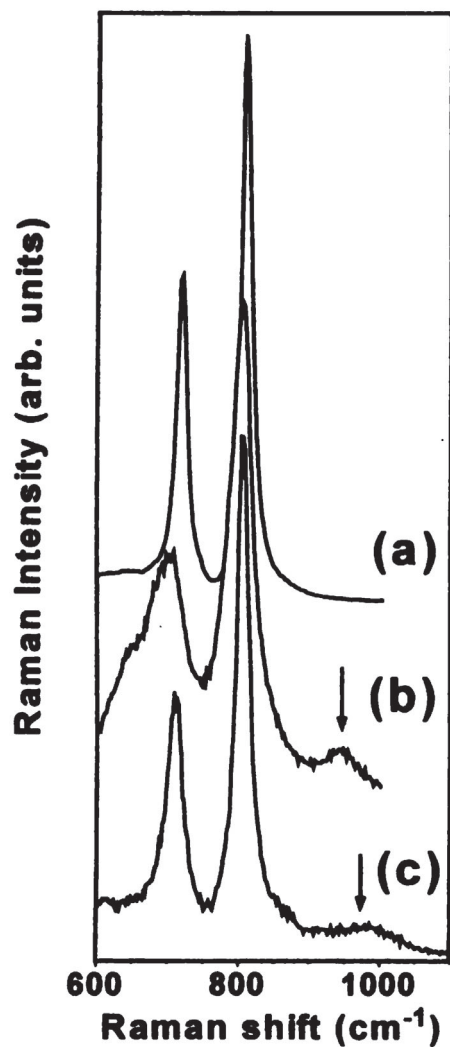


Fig. 8. Raman spectra of high-frequency stretching modes in (a) "virgin"  $\text{WO}_3$  powder, (b) pure  $\text{WO}_3$  powder ground for 21 h, (c) mixed sample with  $x = 0.1$ . The low intensity Raman band at  $950 \text{ cm}^{-1}$  in (b) and  $980 \text{ cm}^{-1}$  in (c) is attributed to the presence of short and strong W-O bonds.